CRYSTAL GROWTH & DESIGN

pubs.acs.org/crystal

Article

Incorporating Highly Anisotropic Four-Coordinate Co(II) Ions within One-Dimensional Coordination Chains

Published as part of a Crystal Growth and Design virtual special issue on Molecular Magnets and Switchable Magnetic Materials

Tao Long, Jiong Yang, Shruti Moorthy, Dong Shao,* Saurabh Kumar Singh,* and Yuan-Zhu Zhang*

Cite This: *Cryst. Growth Des.* 2023, 23, 2980−2987

Read Online

ACCESS | Metrics & More | Article Recommendations | Supporting Information

ABSTRACT: Low-coordinate metallic ions have been well recognized for constructing good-performance single ion magnets (SIMs) due to their enhanced magnetic anisotropy; however, the incorporation of such specific ions into coordination polymers is still challenging. Here, we reported two new Co^{II} coordination polymers, namely $[Co(pdms)(bpe)]_n$ (**1**) and $\{[Co(pdms)(tpb)]\cdot H_2O\cdot tpb\}_n$ (**2**) (H_2pdms = 1,2-bis(methanesulfonamido)benzene, bpe = 1,2-di(4-pyridyl)ethane, tpb = 1,2,4,5-tetra(4-pyridyl)benzene). Single crystal X-ray diffraction experiments indicated that the Co^{II} centers in both **1** and **2** display a distorted tetrahedral geometry with quasi C_{2v} symmetry and are linked into a one-dimensional (1D) *zig-zag* chain via the ditopic bridging ligand of bpe in **1** while a ribbon chain via the tetradentate linker of tpb in **2**. Magnetic studies revealed the easy-axis magnetic anisotropy of the Co^{II} ions with different zero-field splitting D of -19 cm^{-1} (**1**) and -33 cm^{-1} (**2**), likely due to the distinct changes in the $N_{py}-Co-N_{py}$ bite angles (100.20° (**1**) vs. 93.90° (**2**)). Moreover, slow magnetic relaxation proceeded via different relaxation mechanisms under applied dc fields was observed, giving an effective energy barrier (U_{eff}) of 69.6 K for **1** and 76.6 K for **2**, respectively. The *ab initio* calculations on both the polymers further confirmed the sign and magnitude of the ZFS parameters and nicely reproduced the experimental results. Our study demonstrated a great potential for applying the well-studied and highly anisotropic 4-coordinate metal ions within a coordination polymer, opening a viable means to tuning magnetic anisotropy via topological control.

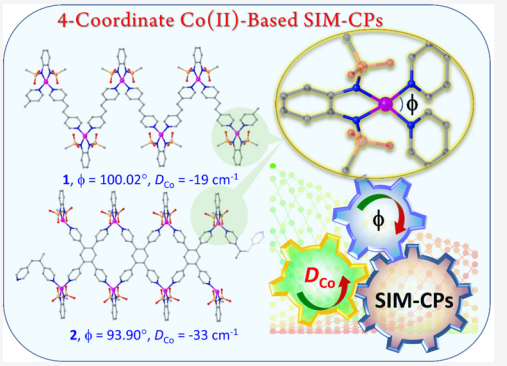

INTRODUCTION

Single-molecule magnets (SMMs) are molecules of nanoscale that show slow magnetic relaxation of purely molecular origin.[1] Having developed over decades, thousands of SMMs have been synthesized and characterized to display a variety of magnetic complexes with distinct barrier (U_{eff}) and magnetic blocking temperatures (T_B).[2] One of the milestones in this field is that a mononuclear Fe^{II} complex was observed to display slow magnetic relaxation in 2010 by Long et al.,[3] which greatly prompted the search of new monometallic transition-metal-based SMMs (also termed single-ion magnets, SIMs).[4] With the characterization of a high-performance organometallic Er(III) SIM reported by Gao and co-workers,[5] the design principles from multinuclear SMMs to SIMs were basically established, and the field of SIMs has then entered a stage of rapid development. To date, the very best SIM systems were found to be related to the low-coordinate transition-metal ions and organometallic lanthanide complexes within a particular coordination geometry, which can greatly improve the limit of magnetic anisotropy.[6]

Besides the mononuclear complexes, a series of coordination polymers (CPs) or metal−organic frameworks (MOFs),[7] which are built with metal nodes (a single metal ion or a cluster) and organic linking ligands were reported to display slow relaxation of the magnetization under zero filed or applied dc fields.[8−14] Such 3d or 4f complexes can be considered as SIM-CPs or SMM-CPs because magnetically they exhibit the nature of their metal nodes due to negligible internode interactions.[15−19] In fact, they have provided a new platform for manipulating the magnetic dynamics. As an illustrative example, Cano et al. reported the guest-dependent SIM behavior in a family of cobalt(II) MOFs.[9] Our recent studies on some 1D or 2D SIM-MOFs also showed that the magnetic dynamics of such complexes can be tuned by switching the

Received: January 25, 2023
Revised: March 3, 2023
Published: March 13, 2023

https://doi.org/10.1021/acs.cgd.3c00082
Cryst. Growth Des. 2023, 23, 2980−2987

Scheme 1. Molecule Structures of $[Co(pdms)_2]^{2-}$ Building Unit, the Bridging Ligands bpe and tpb, and the Resulting Topology Structures of 1 and 2

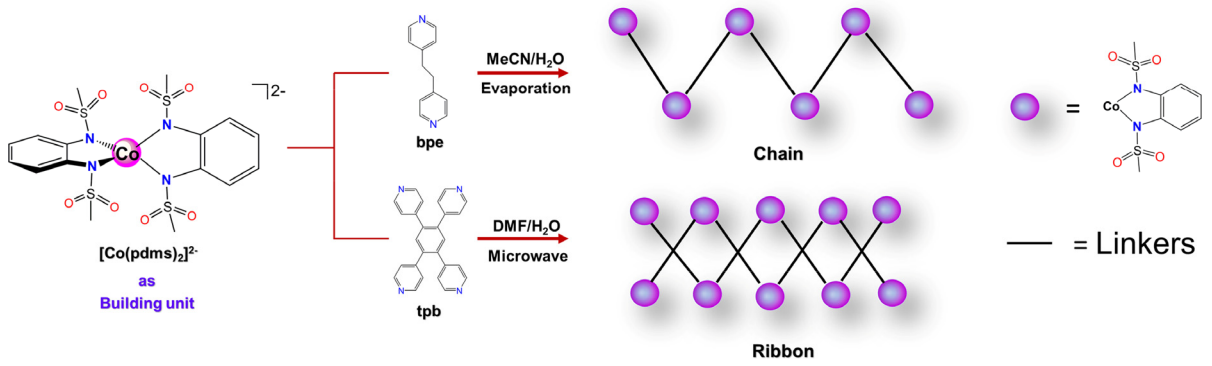

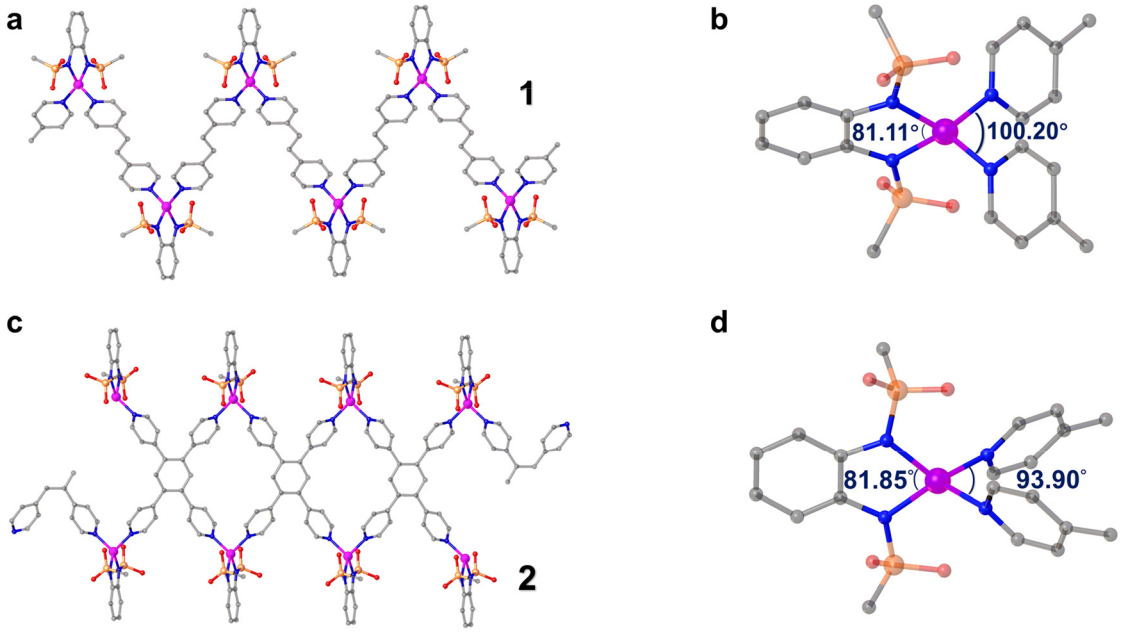

Figure 1. Structural representation of the 1D zigzag chain structure of **1** (a) and 1D ribbon structure of **2** (c). Local coordination environments of the Co^{2+} ions in **1** (b) and **2** (d). Color code: Co, purplish red; S, orange; O, red; N, blue; C, black. Hydrogen atoms or solvent molecules are omitted for clarity. Symmetry codes: 1 + *X*, 3/2 − *Y*, 3/2 − *Z*; 2 2 − *X*, 2 − *Y*, 1 − Z for **1**; ^{1}1 + X, +Y, +Z for **2**.

guest molecules, or varying the axial coordination atoms.[10−14] To date, however, the majority of such complexes, including discrete polynuclear complexes, are built with the six-coordinate and octahedral metal centers (Table S1, Table S2, SI) rather than the well-recognized highly anisotropic metal ions, including the low-coordinate ones.[20−22] One major reason lies in the synthetic challenge for preserving/realizing the selected particular geometries within a framework.[23,24]

Previously, Slageren and co-workers reported a remarkable Co(II)-SIM $(HNEt_3)_2[Co(pdms)_2]$ (Scheme 1, H_2pdms = 1,2-bis(methanesulfonamido)benzene), in which the cobalt ion adopts a four-coordinate D_{2d} symmetry and possesses a huge zero-field splitting (ZFS) *D* value of −115 cm^{-1}.[25] Later, they applied such particular geometric ions into a dinuclear SMM via a radical bridge, resulting in a 350-fold increase of the magnetization relaxation time.[26−28] Moreover, this highly stable and anionic molecule was able to cocrystallize with other functional components for realizing multifunctionalities, such as magnetic bistability and conductivity.[29−31] Very recently, we found that as long as nitrogen-containing organic ligands are present, $[Co(pdms)_2]^{2-}$ dianionic molecules form stable neutral species, and importantly, the coordination geometry is nearly preserved.[32] Along this line, herein, we utilized two different organic linkers and achieved the preparation of two coordination complexes, $[Co(pdms)(bpe)]_n$ (**1**) and $\{[Co(pdms)(tpb)]\cdot H_2O\cdot tpb\}_n$ (**2**) (Scheme 1, bpe = 1,2-di(4-pyridyl)ethane, tpb = 1,2,4,5-tetra(4-pyridyl)benzene). A single crystal X-ray diffraction study indicated that the Co^{2+} centers in both **1** and **2** display a distorted tetrahedral geometry (C_{2v} symmetry) and are linked into a one-dimensional (1D) zig-zag chain via the ditopic bridging ligand of bpe in **1** while a ribbon chain via the tetradentate linker of tpb in **2**. Interestingly, magnetic measurements revealed that both **1** and **2** showed the field-induced SIM behaviors with the evidenced easy-axis magnetic anisotropy, the different magnitudes of which were likely regulated by the distinct N_{py}−Co−N_{py} bite angles. Theoretical calculations were used to analyze the difference in the magnetic properties of **1** and **2**, providing insight into the design of potential high-performance SIM-CPs.

https://doi.org/10.1021/acs.cgd.3c00082
Cryst. Growth Des. 2023, 23, 2980−2987

RESULTS AND DISCUSSION

Synthesis and Crystal Structures. As observed previously, the $[Co(pdms)_2]^{2+}$ species becomes labile and may form a relatively stable neutral {Co(pdms)} component with the existence of pyridinyl derivatives.[32] As such, the pure crystalline sample of **1** was prepared directly through the reaction of $[Co(pdms)_2]^{2+}$ and the organic pyridine derivative of bpe. Due to the bad solubility of the bulk tpb ligand, a one-pot microwave solvothermal method was successfully employed for the synthesis of **2**. Both **1** and **2** crystallize cleanly as dark red block crystals in high yields. Experiments with powder X-ray diffraction (PXRD) confirmed the purities of bulk crystalline samples **1** and **2**, and the experimental PXRD patterns are basically consistent with the simulated patterns (Figure 1, SI). Notably, we can see relatively major differences for **2**, which may be due to the loss of crystallization water molecules during the grinding process. Furthermore, thermogravimetric analysis (TGA, Figure S2, SI) revealed that the mass of **1** remained unchanged up to ca. 260 °C, while a one-step desolvation process below 90 °C with the weight loss of 2.5% (calc. 2.4%) was observed for **2**, which started decompose at ca. 400 °C. This result indicated that the coordination chains for both **1** and **2** are stable.

Single crystal X-ray diffraction analyses reveal the orthorhombic *Pnna* space group of **1**. The asymmetric unit consists of half of one [Co(pdms)(bpe)] unit (Table 1, Figure S3, SI).

Table 1. Crystallographic Data and Structure Refinement Parameters for Complexes 1 and 2

Parameter	1	2
Formula	$C_{20}H_{22}CoN_4O_4S_2$	$C_{34}H_{30}CoN_6O_5S_2$
Formula weight [g mol^{-1}]	505.46	725.69
Crystal system	orthorhombic	triclinic
Space group	*Pnna*	$P\bar{1}$
a [Å]	10.9568(3)	9.2703(5)
b [Å]	15.2587(4)	9.9725(5)
c [Å]	12.6151(4)	18.7745(9)
α [°]	90	77.614(2)
β [°]	90	75.781(2)
γ [°]	90	86.984(2)
V [Å^3]	2109.07(10)	1643.33(15)
Z	4	2
ρ_{calcd} [g cm^{-3}]	193	153
μ(Mo−Kα) [mm^{-1}]	1.592	1.467
F(000)	1.048	0.701
R_{int}	1044.0	750.0
R_1[a]/wR_2[b] ($I > 2\sigma(I)$)	0.0274/0.0747	0.0488/0.1108
R_1/wR_2 (all data)	0.0311/0.0787	0.0817/0.1272
GOF on F_2	1.061	1.041
max/min [e Å^{-3}]	0.46/−0.42	0.63/−0.55

[a] $R_1 = \sum||F_o| - |F_c||/\sum|F_o|$. [b] $wR_2 = \{\sum[w(F_o^2 - F_c^2)^2]/\sum[w(F_o^2)^2]\}^{1/2}$.

The coordination **1** is a 1D coordination polymer with a zigzag chain topology. The neutral {Co(pdms)} units are linked by each end of the nitrogen atoms of bpe ligands (Figure 1). In the chain, the Co^{II} centers are distorted tetrahedrons made up of two nitrogen atoms from bpe and two nitrogen atoms from pdms (Figure 1b). Complex **2** crystallizes in the triclinic $P\bar{1}$ space group and has a 1D ribbon topology (Table 1, Figure 1c). The asymmetric unit of **2** contains a complete {Co(pdms)} moiety and half of a coordinated tpb ligand and half of a crystallize lattice tpb ligand (Figure S3, SI). The cobalt centers in **2** are chelated by four N atoms from one pdms and two tetradentate tpb ligands and linked through cis-disposed nitrogen atoms of the tpb linkers (Figure 1d), giving a 1D ribbon coordination polymer with tetrahedral Co^{II} centers. As shown in Tables S2 and S3, selected bond lengths and angles for **1** and **2** are summarized.

The structural characteristics are worth further comparing to unveil the magneto-structural relationship. The average Co−N bond distances in **1** and **2** are 1.999 and 2.003 Å, respectively, which is comparable with the bond distances in the parent complex (Figure S4, SI). The almost same bond distances in **1** and **2** can carefully exclude the effective influence of the bond distance on magnetic anisotropy. The continuous shape measure (CSM) values for **1** and **2** calculated by SHAPE 2.1[33] are 3.312 and 3.733 (Table S4, SI), respectively, indicating a large distortion from standard tetrahedral geometry (CSM = 0). For tetrahedral mononuclear cobalt complexes, except for the bond distance and structural distortion, the ∠N−Co−N bite angle has vital significance in the zero-field splitting parameter D, which has been established by experimental and computational studies.[34−37] Thus, the ∠N−Co−N bite angles of the Co^{II} ions in **1** and **2** were compared (Figure 1b,d). As can be seen, one of the ∠N−Co−N bite angles (81.11° and 81.85°) supported by the pdms ligand is close to the angle (80.70° and 80.59°) in the parent complex (Figure S3, SI). However, another ∠N−Co−N bite angle chelated the Co^{II} ion by two neighboring bpe ligands, and two tpb ligands are 100.20° and 93.90° for **1** and **2**, respectively (Figure 1b,d). These unique cheating modes with distinct N−Co−N bite angles are very rare in the family of distorted tetrahedral Co(II) complexes.[34−44] The overall crystal packing structure of **1** and **2** indicates a well-isolated Co^{II} ion from a magnetic perspective with the shortest interchain and intrachain Co···Co distances being 11.416 Å and 8.388 for **1** and 12.194 Å and 9.972 for **2** (Figure S5, SI). These separations are larger than most reported values in 1D Co(II) coordination polymers (Table S1, SI) and relatively long, making it unlikely that there will be potential intermolecular magnetic interaction.

Static Magnetic Properties. Temperature-dependent magnetic susceptibility data were measured for **1** and **2** in the temperature range of 2−300 K under a dc field of 1 kOe (Figure 2). The $\chi_M T$ values at 300 K for **1** and **2** are 2.82 and 2.32 cm^3 mol^{-1} K, respectively, larger than the spin-only value of 1.875 cm^3 mol^{-1} K for a high-spin Co^{II} ion ($S = 3/2$, $g = 2$), suggesting a significant orbital contribution originating from a low-lying electronic excited state coupled to the ground electronic state through spin−orbit coupling (SOC) of the high-spin Co^{II} ions in a distorted T_d symmetry to the magnetic momentum. For **1** and **2**, the $\chi_M T$ values remain essentially constant from 300 to 50 K, where the curves begin to decrease monotonously down to 1.71 and 1.66 cm^3 mol^{-1} K, respectively. Other reported mononuclear Co(II) complexes with distorted tetrahedral geometry also show similar curves.[34−44] In stark comparison, the values of $\chi_M T$ in the measured temperature range for **2** are notably larger than the values of **1**, supporting the important effect of the ∠N−Co−N bite angle on magnetic properties and indicating a larger magnetic anisotropy of the Co^{II} ion in **2**. Also, different temperatures were used to measure the field-dependent magnetization curves of **1** and **2** (Figure S6, SI). For a high-spin Co^{II} ion with $S = 3/2$ and $g = 2.0$, the magnetization

https://doi.org/10.1021/acs.cgd.3c00082
Cryst. Growth Des. 2023, 23, 2980−2987

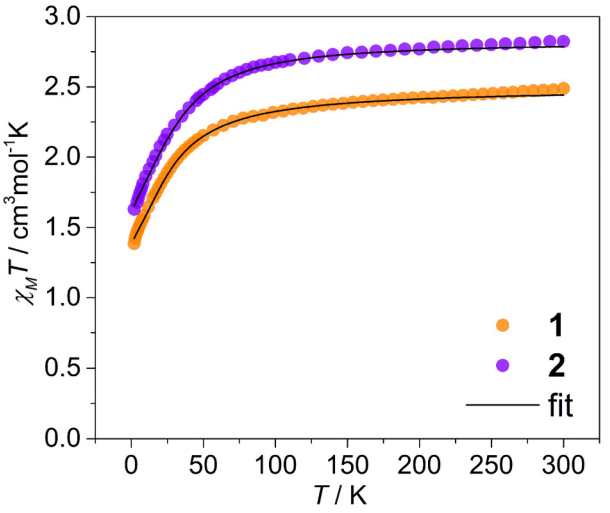

Figure 2. Magnetic susceptibilities of **1** and **2** measured at 1 kOe. Solid lines are best fits by PHI.

values at 7 T and 2 K are 2.21 and 2.18 μ_B, which are far below the saturation value of 3 μ_B. Insufficiency of the saturation reveals the hallmarks of significant magnetic anisotropy in **1** and **2**.

Magnetically, though **1** and **2** are coordination polymers with distinct 1D topologies, the Co^{II} centers are bridged by various long organic ligands, giving rise to two magnetically noninteracting Co^{II} centers in **1** and **2**. These coordination polymers with negligible magnetic interactions between the metal centers can still be treated as single-ion systems.[9−14] To estimate the zero-field splitting (ZFS) parameters (D, E, g tensors) of **1** and **2**, the susceptibility and magnetization data in the measured temperature range were simultaneously fitted by the *PHI* program[40] considering the following spin Hamiltonian:

$$\hat{H} = D\left[\hat{S}_z - \frac{\hat{S}(\hat{S}+1)}{3}\right] + E(\hat{S}_x^2 - \hat{S}_y^2) + \mu_B g\cdot\hat{S}\cdot B \quad (1)$$

where D, E, S, μ_B, and B represent the axial and rhombic ZFS parameters, the spin operator, Bohr magneton, and magnetic field vectors, respectively. The best fits afford D = −21.1 cm^{-1}, $|E/D|$ = 0.12, g = 2.457 for **1**, and D = −35.3 cm^{-1}, $|E/D|$ = −0.16, g = 2.621 for **2**. Hence, there is an easy-axis magnetic anisotropy of the distorted tetrahedral Co^{II} centers in compounds **1** and **2** as indicated by these negative D values. The magnitude of the D values is comparable with structurally similar four-coordinate Co(II) complexes.[32,43] Furthermore, complex **1** has a larger D value than complex **2**, indicating a greater magnetic anisotropy. For mononuclear tetrahedral Co^{II} complexes, magnetic anisotropy has been found to correlate with several factors, including different first coordination spheres (Heavy atom effect), second coordination spheres (Ligands effect),[40,43] structural disorder (solid-state effects),[44] and the N−Co−N bite angle.[34−37] On the basis of structural analyses, the most notable effect on magnetic properties, including magnetic anisotropy and relaxation dynamics, should be the N−Co−N bite angle modified through a topology control by molecular design. From the experiments and theoretical studies, the small ∠N−Co−N bite angle will lead to a relatively large magnitude of D value.[38,39,45] In addition, nonlinear dependency between the ∠N−Co−N bite angle and the splitting of d-orbitals was also observed in some four-coordinated Co(II) complexes.[41−44]

Dynamic Magnetic Properties. The parent Co(II) complex is a high-performance zero-field SIM, and thus temperature- and frequency-dependent ac susceptibility measurements were measured to probe the potential SIM behavior in compounds **1** and **2**. For their considerable magnetic anisotropy of the Co^{2+} ions in compounds **1** and **2**, the well-isolated Co^{2+} centers, in principle, can exhibit slow magnetization relaxation.[41−44] However, both the polymers do

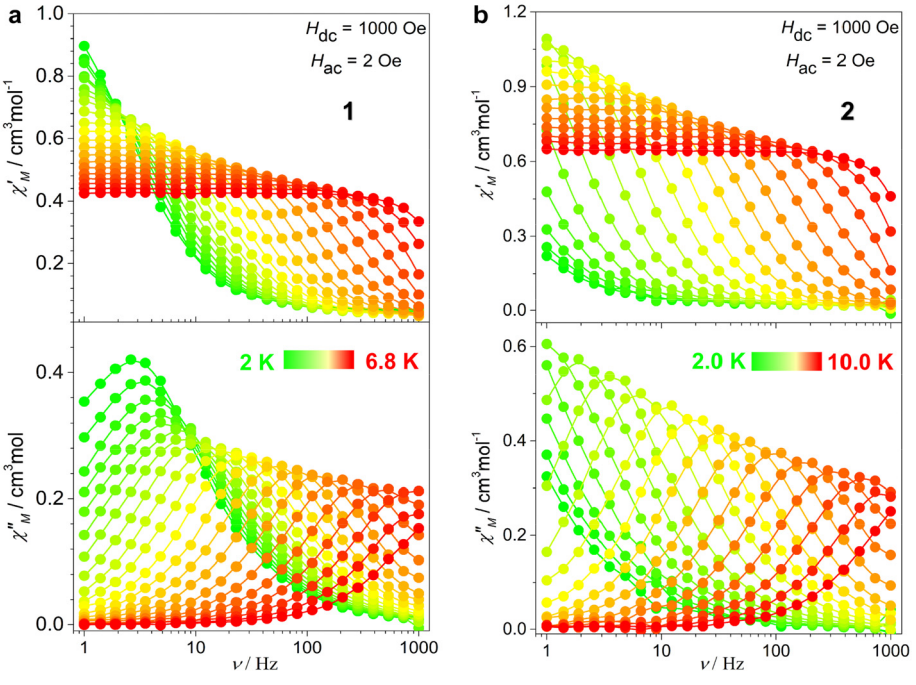

Figure 3. Ac magnetic susceptibilities of in-phase (χ') and out-of-phase (χ'') parts measured under various temperatures for **1** (a) and **2** (b).

https://doi.org/10.1021/acs.cgd.3c00082
Cryst. Growth Des. 2023, 23, 2980−2987

not display out-of-phase (χ'') ac magnetic susceptibility signals (Figure S7, SI). A similar scenario also happened in our recently reported binuclear cobalt(II) metallocycle, in which the lack of zero-field SMM behavior originates from a small negative D value but significantly large rhombic contribution.[32] Additionally, normal spin flip and/or quantum tunnelling of magnetization (QTM) relaxation induced by hyperfine interactions and dipolar interactions are potential reasons accounting for this. Generally, the application of small dc fields during the ac measurements can eliminate the QTM and induce the happening of slow magnetic relaxation. Additionally, a 1 kOe dc field was the most used optimum field for the suppression of QTM, especially for cobalt complexes.[11−22,46−49] For compounds **1** and **2**, temperature- and frequency-dependent ac susceptibility signals were observed when the 1 kOe dc field was applied (Figure 3, Figure S8, SI). These results support two SIM-CPs of compounds **1** and **2**. Notably, these two coordination polymers are unique among the family of 1D SIM-CPs (Table S1, SI) because of the rigid zigzag chain structure of **1** and the unprecedented SIM ribbon of **2**. At 2 K, the peak of χ'' signal of **1** appeared, while for **2** it can be observed until the temperature rises to ca. 3 K, revealing a "slower" magnetic relaxation.

The relaxation times of compounds **1** and **2** at each temperature were extracted from the fitting of the frequency dependence of the χ'' vs χ' signals (Cole−Cole plots, Figure S9, SI) by using the generalized Debye model.[50] The obtained α values are in the range of 0.01−0.17 and 0.02−0.08 for compounds **1** and **2** (Table S5, S6, SI), respectively. Then, the inverse relaxation time τ^{-1} vs temperature plots for compounds **1** and **2** were drawn (Figure 4). To obtain Orbach process

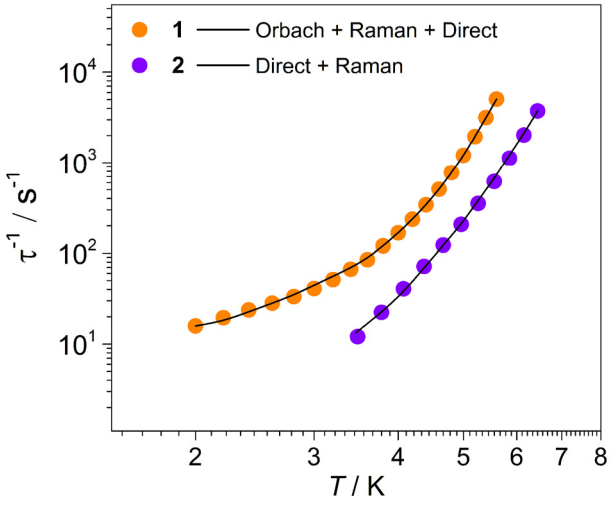

Figure 4. Inverse relaxation time vs temperature plot for **1** (2.0−5.6 K) and **2** (3.4−6.4 K). The black lines represent the fits via the combined Direct and Raman, and the QTM, Direct, and Raman relaxation mechanisms for **1** and **2**, respectively.

related parameters, the high-temperature extracted relaxation times for compounds **1** and **2** were fitted to an Arrhenius law $\tau = \tau_0 \cdot \exp(U_{eff}/k_BT)$ (Figure S10, SI), affording an effective energy barrier (U_{eff}) of 70(1) K and a pre-exponential factor (τ_0) of $8.0(1) \times 10^{-10}$ s for complex **1** and $U_{eff} = 77(5)$ K, and $\tau_0 = 1.8(6) \times 10^{-9}$ s for **2**. From these results, it is obvious that the U_{eff} of **1** is significantly larger than the expected energy gap ($|2D| = 56.2$ K for **1**) based on experimental magnetic data. However, the U_{eff} of **2** is lower than the experimental energy gap of 97.3 K of **2**. Due to the Orbach process that takes place between real magnetic energy levels, for **1** the Orbach relaxation can proceed, while the relaxation should not happen in **2**.

To further probe the magnetic relaxation processes, the τ^{-1} vs T data of **1** and **2** were analyzed by CC-FIT2 program.[51] The nonlinear T dependence of the τ reveals that multiple relaxation pathways should be responsible to the relaxation mechanisms.[52,53] For single-ion systems, four possible relaxation mechanisms can be considered, including QTM, Direct, Raman, and Orbach mechanisms. The sum of the four relaxation processes can be modeled by the following equation:

$$\tau^{-1} = {\tau_{QTM}}^{-1} + AT + CT^n + {\tau_0}^{-1} \exp\left(-\frac{U_{eff}}{k_BT}\right) \quad (2)$$

where the terms correspond to QTM, Direct, Raman, and Orbach processes, respectively. The τ^{-1} vs T data of **1** was well reproduced by a Direct, Raman, and Orbach model, $\tau^{-1} = AT + CT^n + {\tau_0}^{-1} \cdot \exp(-U_{eff}/k_BT)$. The best-fit parameters are $U_{eff} = 63(2)$ K, $\tau_0 = 10^{-8(7)}$ s, $A = 0.2(1)$ s^{-1} K^{-1}, $C = 10^{-0.2(1)}$ s^{-1} K^{-n}, and $n = 4.1(2)$ (Figure 4). These results provide another proof to support a Orbach relaxation that happened in **1**. For complex **2**, the temperature dependence of the relaxation times was nicely fitted by a Direct and Raman model ($\tau^{-1} = AT + CT^n$), giving $A = 0.06(1)$ s^{-1} K^{-1}, $C = 3.8(6) \times 10^{-2}$ s^{-1} K^{-n}, and $n = 6.2(1)$ (Figure 4). The Raman relaxation process in **1** and **2** was supported by the fitted n values that are in a reasonable range of 1−9. From these results, the structural topologies not only can modify the magnetic anisotropy via changing the local geometries but also are of importance for the magnetic relaxation dynamics.

Theoretical Studies. To further determine the sign and magnitude of the ZFS splitting in complexes **1** and **2**, here we have prepared the mononuclear model complex and performed *ab initio* calculations (see Supporting Information for the details). Complete active space self-consistent field (CASSCF) followed by second-order N-electron valence perturbation theory (NEVPT2) was carried out on model complexes with an active space of CAS(7,5) to compute the spin-Hamiltonian parameters (Table S7, S8, SI). This methodology has been widely used to compute the spin-Hamiltonian (SH) parameters in various open-shell transition metal complexes.[32,54] NEVPT2 (CASSCF) computed D values are −29.6(−32.8) cm^{-1} and −31.6(−34.8) cm^{-1} for complexes **1** and **2** respectively. The computed E/D values are 0.05(0.06) and 0.04(0.04) for complexes **1** and **2**, respectively, at the NEVPT2(CASSCF) level of theory (Table 2, Figure S9, SI). Calculations show an easy axis of anisotropy for both complexes with negligible rhombicity. NEVPT2 computed effective g-tensors are $g_{xx} = 2.121$, $g_{yy} = 2.151$, $g_{zz} = 2.501$ and $g_{xx} = 2.124$, $g_{yy} = 2.144$, $g_{zz} = 2.524$ for complexes **1** and **2**

Table 2. NEVPT2 Computed Spin-Hamiltonian Parameters (along with Experimental Values in Brackets) for Complexes 1 and 2

	D	$\lvert E/D \rvert$	g_{min}	g_{mid}	g_{max}
1	−29.6	0.05	2.121	2.151	2.501
	(−21.1)	(0.12)	(2.013)	(2.138)	(2.616)
2	−31.6	0.06	2.124	2.144	2.524
	(−35.3)	(0.16)	(2.128)	(2.191)	(2.797)

https://doi.org/10.1021/acs.cgd.3c00082
Cryst. Growth Des. 2023, 23, 2980−2987

respectively, which further supports the finding of the negative D value ($g_{zz} > g_{xx}$; g_{yy}; Table S9, SI). The computed D-tensor orientation for both complexes is provided in Figure 5. The

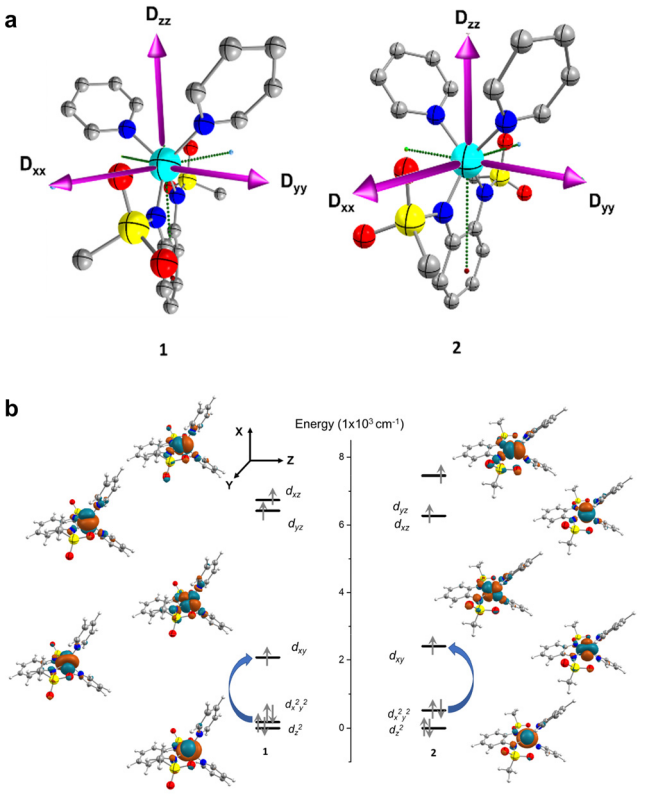

Figure 5. (a) NEVPT2 computed orientation of a D-tensor for **1** and **2**. Hydrogens have been omitted for clarity. Color code: Co (cyan); N (blue), O (red), S (yellow), C (gray). (b) Ab initio ligand field theory (AILFT) computed d-orbital ordering for **1** (left) and **2** (right).

computed D-tensor passes nearly through the C_2 axis, which bisects the bpe and tpb ligands in complex **1** and **2**, respectively. Our computed SH parameters nicely reproduce the experimental *dc* magnetic susceptibility data, which confirms the validity of our computational methodology (Figure S12, SI).

For both complexes, the sign of the D values is negative, with a relatively large magnitude for complex **2**. Both the model complexes **1** and **2** have differed in terms of the ∠N−Co−N bite angle of the bpe and tpb ligands as the ∠N−Co−N bite angle of pdms ligand is nearly same (Figure S13, SI). The ∠N−Co−N bond angle in complexes **1** (**2**) is ∼100.2° (∼93.9°) respectively, representing a tetragonally elongated geometry. Our previously developed magentostructural correlations show that D values are always negative for the tetragonally elongated complexes as the constrained ∠N−Co−N bond angle brings the d_{xy} and $d_{x^2-y^2}$ orbitals ($m_l = \pm 2$) much closer to each other, which ensures the lowest excitation between the same m_l level.[32] (see the computed AILFT orbital ordering in Figure 5b, SI). Mapping of the structural parameters of complex **1** and **2** on the previously developed magnetostructural correlations yields a D value of −26.5 (−34.8) cm^{-1}, which matches excellently with the experimental and computed data (Figure S14, SI). This highlights the robustness of the developed magneto-structural correlations in predicting the sign and magnitude of the D values in tetrahedral Co(II) complexes.

CONCLUSIONS

In summary, we have successfully isolated two rare Co(II) coordination polymers with different 1D topologies (zigzag for **1** vs. ribbon for **2**) based on the highly anisotropic 4-coordinate cobalt centers. Both experimental and theoretical studies revealed that the local Co(II) ion adopting distorted a tetrahedral geometry with the quasi C_{2v} symmetry is uniaxially anisotropy in magnetization along its C_2 axis, and its magnitude is highly dependent on the N_{py}−Co−N_{py} bite angles. Remarkably, both **1** and **2** exhibited the typical field-driven SIM behaviors with the effective energy barrier being 69.6 K for **1** and 76.6 K for **2**, respectively. The foregoing result thus provides a unique example of assembling a well-recognized and highly anisotropic metal ions as a node within a coordination polymer. Further efforts are underway to realize higher dimensional MOFs with this particular building unit and introduce radical linkers instead of the current diamagnetic ones.

ASSOCIATED CONTENT

Supporting Information

The Supporting Information is available free of charge at https://pubs.acs.org/doi/10.1021/acs.cgd.3c00082.

Experimental details, results of CSM analysis, PXRD, TGA, and additional structural views and structure parameters for **1** and **2**. The computational details, CASSCF, NEVPT2 computed spin-free, spin−orbit energies, spin-Hamiltonian parameters for complexes **1** and **2** (PDF)

Accession Codes

CCDC 2179379−2179380 contain the supplementary crystallographic data for this paper. These data can be obtained free of charge via www.ccdc.cam.ac.uk/data_request/cif, or by emailing data_request@ccdc.cam.ac.uk, or by contacting The Cambridge Crystallographic Data Centre, 12 Union Road, Cambridge CB2 1EZ, UK; fax: +44 1223 336033.

AUTHOR INFORMATION

Corresponding Authors

Yuan-Zhu Zhang − *Department of Chemistry, Southern University of Science and Technology (SUSTech), Shenzhen 518055, China;* orcid.org/0000-0002-1676-2427; Email: zhangyz@sustech.edu.cn

Saurabh Kumar Singh − *Department of Chemistry, Indian Institute of Technology Hyderabad, 502285 Sangareddy, Telangana, India;* orcid.org/0000-0001-9488-8036; Email: sksingh@chy.iith.ac.in

Dong Shao − *Hubei Key Laboratory of Processing and Application of Catalytic Materials, College of Chemistry and Chemical Engineering, Huanggang Normal University, Huanggang 438000, P. R. China;* orcid.org/0000-0002-3253-2680; Email: shaodong@nju.edu.cn

Authors

Tao Long − *Hubei Key Laboratory of Processing and Application of Catalytic Materials, College of Chemistry and Chemical Engineering, Huanggang Normal University, Huanggang 438000, P. R. China*

https://doi.org/10.1021/acs.cgd.3c00082
Cryst. Growth Des. 2023, 23, 2980−2987

Jiong Yang − *Department of Chemistry, Southern University of Science and Technology (SUSTech), Shenzhen 518055, China*

Shruti Moorthy − *Department of Chemistry, Indian Institute of Technology Hyderabad, 502285 Sangareddy, Telangana, India*

Complete contact information is available at: https://pubs.acs.org/10.1021/acs.cgd.3c00082

Notes

The authors declare no competing financial interest.

■ ACKNOWLEDGMENTS

This work was supported by Huanggang Normal University (Nos. 2042021033, 202210204), Young Talents Project of Department of Education of Hubei Province (No. Q20222904), the Open Foundation of Hubei Key Laboratory of Novel Reactor and Green Chemical Technology (No. NRGC202210), and the Open Foundation of State Key Laboratory of Coordination Chemistry (SKLCC2208). Y.Z.Z. acknowledges the financial support of the Stable Support Plan Program of Shenzhen Natural Science Fund (No. 20200925151834005) and the National Natural Science Foundation of China (No. 22173043). S.K.S. acknowledges the Department of Science and Technology for the Start-up Research Grant (SRG/2020/001323) and IIT Hyderabad for generous funding. S.M. acknowledges a PMRF fellowship. The support and resources provided by PARAM Seva, IIT Hyderabad are gratefully acknowledged.

■ REFERENCES

(1) Gatteschi, D.; Sessoli, R.; Villain, J. *Molecular Nanomagnets*; Oxford University Press: Oxford, 2006.

(2) Shao, D.; Wang, X.-Y. Development of single-molecule magnets. *Chin. J. Chem.* **2020**, *38*, 1005−1018.

(3) Freedman, D. E.; Harman, W. H.; Harris, T. D.; Long, G. J.; Chang, C. J.; Long, J. R. Slow Magnetic Relaxation in a High-Spin Iron(II) Complex. *J. Am. Chem. Soc.* **2010**, *132*, 1224−1225.

(4) Sahu, P. K.; Kharel, R.; Shome, S.; Goswami, S.; Konar, S. Understanding the unceasing evolution of Co(II) based single-ion magnets. *Coord. Chem. Rev.* **2023**, *475*, 214871.

(5) Jiang, S.-D.; Wang, B.-W.; Sun, H.-L.; Wang, Z.-M.; Gao, S. An Organometallic Single-Ion Magnet. *J. Am. Chem. Soc.* **2011**, *133*, 4730−4733.

(6) Bunting, P. C.; Atanasov, M.; Damgaard-Møller, E.; Perfetti, M.; Crassee, I.; Orlita, M.; Overgaard, J.; van Slageren, J.; Neese, F.; Long, J. R. A linear cobalt(II) complex with maximal orbital angular momentum from a non-Aufbau ground state. *Science* **2018**, *362*, eaat7319.

(7) Furukawa, H.; Cordova, K. E.; O'Keeffe, M.; Yaghi, O. M. The chemistry and applications of metal-organic frameworks. *Science* **2013**, *341*, 1230444.

(8) Thorarinsdottir, A. E.; Harris, T. D. Metal−Organic Framework Magnets. *Chem. Rev.* **2020**, *120*, 8716−8789.

(9) Vallejo, J.; Fortea-Pérez, F. R.; Pardo, E.; Benmansour, S.; Castro, I.; Krzystek, J.; Armentano, D.; Cano, J. Guest-dependent single-ion magnet behaviour in a cobalt(II) metal−organic framework. *Chem. Sci.* **2016**, *7*, 2286−2293.

(10) Zhang, X.; Vieru, V.; Feng, X.; Liu, J.-L.; Zhang, Z.; Na, B.; Shi, W.; Wang, B.-W.; Powell, A. K.; Chibotaru, L. F.; Gao, S.; Cheng, P.; Long, J. R. Influence of Guest Exchange on the Magnetization Dynamics of Dilanthanide Single-Molecule-Magnet Nodes within a Metal−Organic Framework. *Angew. Chem., Int. Ed.* **2015**, *54*, 9861−9865.

(11) Shao, D.; Yang, X.; Moorthy, S.; Yang, J.; Shi, L.; Singh, S. K.; Tian, Z. Tuning the structure and magnetic properties via distinct pyridine derivatives in cobalt(II) coordination polymers. *Dalton Trans.* **2022**, *51*, 695−704.

(12) Shao, D.; Moorthy, S.; Peng, P.; Shi, L.; Tang, W.-J.; Wei, X.-Q.; Wang, Z.-J.; Singh, S. K. A Single-Ion Magnet Tape with Five-Coordinate Cobalt(II) Centers. *Eur. J. Inorg. Chem.* **2022**, *2022* (27), e202200354.

(13) Tian, Z.; Moorthy, S.; Xiang, H.; Peng, P.; You, M.; Zhang, Q.; Yang, S.-Y.; Zhang, Y.-L.; Wu, D.-Q.; Singh, S. K.; Shao, D. Tuning chain topologies and magnetic anisotropy in one-dimensional cobalt(II) coordination polymers via distinct dicarboxylates. *CrystEngComm* **2022**, *24*, 3928−3937.

(14) Tang, W.-J.; Wu, S.-T.; Bu, X.-M.; Zhang, H.-Y.; Wei, X.-Q.; Shao, D. Field-induced single-ion magnet behavior in a cobalt(II) coordination polymer constructed by a mixed bipyridyl-tetracarboxylate strategy. *Polyhedron* **2023**, *229*, 116175.

(15) Huang, X.-D.; Ma, X.-F.; Zheng, L.-M. Photo-responsive Single-Molecule Magnet Showing 0D to 1D Single-Crystal-to-Single-Crystal Structural Transition and Hysteresis Modulation. *Angew. Chem., Int. Ed.* **2023**, e202300088.

(16) de Oliveira Maciel, J. W.; Lemes, M. A.; Valdo, A. K.; Rabelo, R.; Martins, F. T.; Queiroz Maia, L. J.; de Santana, R. C.; Lloret, F.; Julve, M.; Cangussu, D. Europium(III), Terbium(III), and Gadolinium(III) Oxamato-Based Coordination Polymers: Visible Luminescence and Slow Magnetic Relaxation. *Inorg. Chem.* **2021**, *60*, 6176−6190.

(17) Fang, Y.; Sun, R.; Sun, A.-H.; Sun, H.-L.; Gao, S. The construction of dynamic dysprosiumcarboxylate ribbons by utilizing the hybrid-ligand conception. *Dalton Trans.* **2021**, *50*, 1246−1252.

(18) Bazhenova, T. A.; Mironov, V. S.; Yakushev, I. A.; Svetogorov, R. D.; Maximova, O. V.; Manakin, Y. V.; Kornev, A. B.; Vasiliev, A. N.; Yagubskii, E. B. End-to-End Azido-Bridged Lanthanide Chain Complexes (Dy, Er, Gd, and Y) with a Pentadentate Schiff-Base $[N_3O_2]$ Ligand: Synthesis, Structure, and Magnetism. *Inorg. Chem.* **2020**, *59*, 563−578.

(19) Ji, X.-Q.; Xiong, J.; Sun, R.; Ma, F.; Sun, H.-L.; Zhang, Y.-Q.; Gao, S. Enhancing the magnetic performance of pyrazine-N-oxide bridged dysprosium chains through controlled variation of ligand coordination modes. *Dalton Trans.* **2021**, *50*, 7048−7055.

(20) Kharwar, A. K.; Mondal, A.; Konar, S. Alignment of axial anisotropy of a mononuclear hexa-coordinated Co(II) complex in a lattice shows improved single molecule magnetic behavior over a 2D coordination polymer having a similar ligand field. *Dalton Trans.* **2021**, *50*, 2832−2840.

(21) Mondal, A. K.; Khatua, S.; Tomar, K.; Konar, S. Field-Induced Single-Ion-Magnetic Behavior of Octahedral Co^{II} in a Two-Dimensional Coordination Polymer. *Eur. J. Inorg. Chem.* **2016**, *2016*, 3545−3552.

(22) Chen, Z.; Yin, L.; Mi, X.; Wang, S.; Cao, F.; Wang, Z.; Li, Y.; Lu, J.; Dou, J. Field-induced slow magnetic relaxation of two 1-D compounds containing six-coordinated cobalt(II) ions: influence of the coordination geometry. *Inorg. Chem. Front.* **2018**, *5*, 2314−2320.

(23) Yao, B.; Zhang, Y.-Q.; Deng, Y.-F.; Li, T.; Zhang, Y.-Z. Series of Benzoquinone-Bridged Dicobalt(II) Single-Molecule Magnets. *Inorg. Chem.* **2022**, *61*, 15392−15397.

(24) Yao, B.; Lu, F.; Gan, D.-X.; Liu, S.; Zhang, Y.-Q.; Deng, Y.-F.; Zhang, Y.-Z. Incorporating Trigonal-Prismatic Cobalt(II) Blocks into an ExchangeCoupled $[Co_2Cu]$ System. *Inorg. Chem.* **2020**, *59*, 10389−10394.

(25) Rechkemmer, Y.; Breitgoff, F. D.; van der Meer, M.; Atanasov, M.; Hakl, M.; Orlita, M.; Neugebauer, P.; Neese, F.; Sarkar, B.; van Slageren, J. A four-coordinate cobalt(II) single-ion magnet with coercivity and a very high energy barrier. *Nat. Commun.* **2016**, *7*, 10467.

(26) Albold, U.; Bamberger, H.; Hallmen, P. P.; van Slageren, J.; Sarkar, B. Strong Exchange Couplings Drastically Slow Down Magnetization Relaxation in an Air-Stable Cobalt(II)-Radical Single-Molecule Magnet (SMM). *Angew. Chem., Int. Ed.* **2019**, *58*, 9802.

(27) Lunghi, A.; Sanvito, S. Multiple spin−phonon relaxation pathways in a Kramer single-ion magnet. *J. Chem. Phys.* **2020**, *153*, 174113.
(28) Damgaard-Møller, E.; Krause, L.; Tolborg, K.; Macetti, G.; Genoni, A.; Overgaard, J. Quantification of the Magnetic Anisotropy of a Single-Molecule Magnet from the Experimental Electron Density. *Angew. Chem., Int. Ed.* **2020**, *59*, 21203−21209.
(29) Shen, Y.; Ito, H.; Zhang, H.; Yamochi, H.; Cosquer, G.; Herrmann, C.; Ina, T.; Yoshina, S. K.; Breedlove, B. K.; Otsuka, A.; Ishikawa, M.; Yoshida, T.; Yamashita, M. Emergence of Metallic Conduction and Cobalt(II)-Based Single-Molecule Magnetism in the Same Temperature Range. *J. Am. Chem. Soc.* **2021**, *143*, 4891−4895.
(30) Shen, Y.; Cosquer, G.; Ito, H.; Izuogu, D. C.; Thom, A. J. W.; Ina, T.; Uruga, T.; Yoshida, T.; Takaishi, S.; Breedlove, B. K.; Li, Z.-Y.; Yamashita, M. An Organic−Inorganic Hybrid Exhibiting Electrical Conduction and Single-Ion Magnetism. *Angew. Chem., Int. Ed.* **2020**, *59*, 2399−2406.
(31) Shen, Y.; Ito, H.; Zhang, H.; Yamochi, H.; Katagiri, S.; Yoshina, S. K.; Otsuka, A.; Ishikawa, M.; Cosquer, G.; Uchida, K.; Herrmann, C.; Yoshida, T.; Breedlove, B. K.; Yamashita, M. Simultaneous manifestation of metallic conductivity and single-molecule magnetism in a layered molecule-based compound. *Chem. Sci.* **2020**, *11*, 11154−11161.
(32) Shao, D.; Moorthy, S.; Zhou, Y.; Wu, S.-T.; Zhu, J.-Y.; Yang, J.; Wu, D.-Q.; Tian, Z.; Singh, S. K. Field-induced slow magnetic relaxation behaviours in binuclear cobalt(II) metallocycle and exchange-coupled cluster. *Dalton Trans.* **2022**, *51*, 9357−9368.
(33) Llunell, M.; Casanova, D.; Cirera, J.; Alemany, P.; Alvarez, S. *SHAPE*, Version 2.1; Universitat de Barcelona, 2013.
(34) Legendre, C. M.; Damgaard-Møller, E.; Overgaard, J.; Stalke, D. The Quest for Optimal 3d Orbital Splitting in Tetrahedral Cobalt Single-Molecule Magnets Featuring Colossal Anisotropy and Hysteresis. *Eur. J. Inorg. Chem.* **2021**, *2021*, 3108−3114.
(35) Tripathi, S.; Vaidya, S.; Ansari, K. U.; Ahmed, N.; Rivière, E.; Spillecke, L.; Koo, C.; Klingeler, R.; Mallah, T.; Rajaraman, G.; Shanmugam, M. Influence of a Counteranion on the Zero-Field Splitting of Tetrahedral Cobalt(II) Thiourea Complexes. *Inorg. Chem.* **2019**, *58*, 9085−9100.
(36) Carl, E.; Demeshko, S.; Meyer, F.; Stalke, D. Triimidosulfonates as Acute Bite-Angle Chelates: Slow Relaxation of the Magnetization in Zero Field and Hysteresis Loop of a Co^{II} Complex. *Chem.—Eur. J.* **2015**, *21*, 10109−10115.
(37) Cui, H.-H.; Lu, F.; Chen, X.-T.; Zhang, Y.-Q.; Tong, W.; Xue, Z.-L. Zero-Field Slow Magnetic Relaxation and Hysteresis Loop in Four-Coordinate Co^{II} Single-Ion Magnets with Strong Easy-Axis Anisotropy. *Inorg. Chem.* **2019**, *58*, 12555−12564.
(38) Vaidya, S.; Shukla, P.; Tripathi, S.; Rivière, E.; Mallah, T.; Rajaraman, G.; Shanmugam, M. Substituted versus Naked Thiourea Ligand Containing Pseudotetrahedral Cobalt(II) Complexes: A Comparative Study on Its Magnetization Relaxation Dynamics Phenomenon. *Inorg. Chem.* **2018**, *57*, 3371−3386.
(39) Mondal, A. K.; Sundararajan, M.; Konar, S. A new series of tetrahedral Co(II) complexes $[CoLX_2]$ (X = NCS, Cl, Br, I) manifesting single-ion magnet features. *Dalton Trans.* **2018**, *47*, 3745−3754.
(40) Yao, X.-N.; Yang, M.-W.; Xiong, J.; Liu, J.-J.; Gao, C.; Meng, Y.-S.; Jiang, S.-D.; Wang, B.-W.; Gao, S. Enhanced magnetic anisotropy in a telluriumcoordinated cobalt single-ion magnet. *Inorg. Chem. Front.* **2017**, *4*, 701−705.
(41) Bruno, R.; Vallejo, J.; Marino, N.; De Munno, G.; Krzystek, J.; Cano, J.; Pardo, E.; Armentano, D. Cytosine Nucleobase Ligand: A Suitable Choice for Modulating Magnetic Anisotropy in Tetrahedrally Coordinated Mononuclear Co^{II} Compounds. *Inorg. Chem.* **2017**, *56*, 1857−1864.
(42) Zhu, Y.-Y.; Liu, F.; Liu, J.-J.; Meng, Y.-S.; Jiang, S.-D.; Barra, A.-L.; Wernsdorfer, W.; Gao, S. Slow Magnetic Relaxation in Weak Easy-Plane Anisotropy: the Case of a Combined Magnetic and HFEPR Study. *Inorg. Chem.* **2017**, *56*, 697−700.
(43) Vaidya, S.; Tewary, S.; Singh, S. K.; Langley, S. K.; Murray, K. S.; Lan, Y.; Wernsdorfer, W.; Rajaraman, G.; Shanmugam, M. What Controls the Sign and Magnitude of Magnetic Anisotropy in Tetrahedral Cobalt(II) Single-Ion Magnets? *Inorg. Chem.* **2016**, *55*, 9564−9578.
(44) Sottini, S.; Poneti, G.; Ciattini, S.; Levesanos, N.; Ferentinos, E.; Krzystek, J.; Sorace, L.; Kyritsis, P. Magnetic Anisotropy of Tetrahedral Co^{II} Single-Ion Magnets: Solid State Effects. *Inorg. Chem.* **2016**, *55*, 9537−9548.
(45) Chilton, N. F.; Anderson, R. P.; Turner, L. D.; Soncini, A.; Murray, K. S. PHI: A powerful new program for the analysis of anisotropic monomeric and exchange-coupled polynuclear d - and f -block complexes. *J. Comput. Chem.* **2013**, *34*, 1164−1175.
(46) Shao, D.; Peng, P.; You, M.; Shen, L.-F.; She, S.-Y.; Zhang, Y.-Q.; Tian, Z. Hydrogen-bonded Framework of a Cobalt(II) Complex Showing Superior Stability and Field-Induced Slow magnetic Relaxation. *Inorg. Chem.* **2022**, *61*, 3754−3762.
(47) Shao, D.; Xu, F.-X.; Yin, L.; Li, H.-Q.; Sun, Y.-C.; Ouyang, Z.-W.; Wang, Z.-X.; Zhang, Y.-Q.; Wang, X.-Y. Fine-Tuning of Structural Distortion and Magnetic Anisotropy by Organosulfonates in Octahedral Cobalt(II) Complexes. *Chin. J. Chem.* **2022**, *40*, 2193−2202.
(48) Deng, Y.-F.; Singh, M. K.; Gan, D.; Xiao, T.; Wang, Y.; Liu, S.; Wang, Z.; Ouyang, Z.; Zhang, Y.-Z.; Dunbar, K. R. Probing the Axial Distortion Effect on the Magnetic Anisotropy of Octahedral Co(II) Complexes. *Inorg. Chem.* **2020**, *59*, 7622−7630.
(49) Yao, B.; Singh, M. K.; Deng, Y.-F.; Wang, Y.-N.; Dunbar, K. R.; Zhang, Y.-Z. Trigonal Prismatic Cobalt(II) Single-Ion Magnets: Manipulating the Magnetic Relaxation Through Symmetry Control. *Inorg. Chem.* **2020**, *59*, 8505−8513.
(50) Cole, K. S.; Cole, R. H. Dispersion and Absorption in Dielectrics I. Alternating Current Characteristics. *J. Chem. Phys.* **1941**, *9*, 341.
(51) Reta, D.; Chilton, N. F. Uncertainty estimates for magnetic relaxation times and magnetic relaxation parameters. *Phys. Chem. Chem. Phys.* **2019**, *21*, 23567.
(52) Jackson, C. E.; Moseley, I. P.; Martinez, R.; Sung, S.; Zadrozny, J. M. A reaction-coordinate perspective of magnetic relaxation. *Chem. Soc. Rev.* **2021**, *50*, 6684−6699.
(53) Zadrozny, J. M.; Atanasov, M.; Bryan, A. M.; Lin, C.-Y.; Rekken, B. D.; Power, P. P.; Neese, F.; Long, J. R. Slow magnetization dynamics in a series of two-coordinate iron(II) complexes. *Chem. Sci.* **2013**, *4*, 125−138.
(54) Moseley, D. H.; Liu, Z.; Bone, A. N.; Stavretis, S. E.; Singh, S. K.; Atanasov, M.; Lu, Z.; Ozerov, M.; Thirunavukkuarasu, K.; Cheng, Y.; Daemen, L. L.; Lubert-Perquel, D.; Smirnov, D.; Neese, F.; Ramirez-Cuesta, A. J.; Hill, S.; Dunbar, K. R.; Xue, Z.-L. Comprehensive Studies of Magnetic Transitions and Spin−Phonon Couplings in the Tetrahedral Cobalt Complex $Co(AsPh_3)_2I_2$. *Inorg. Chem.* **2022**, *61*, 17123−17136.

https://doi.org/10.1021/acs.cgd.3c00082
Cryst. Growth Des. 2023, 23, 2980−2987